A method for the identification of potentially bioactive argon binding sites in protein families

I Hammami, Géraldine Farjot, Mikaël Naveau, Audrey Rousseaud, Thierry Prangé, Ira Katz, Nathalie Colloc'h

A method for the identification of potentially bio-active argon binding sites in protein families

Islem Hammami,[†,‡] Géraldine Farjot,[‡] Mikaël Naveau,[§] Audrey Rousseaud,[‡] Thierry Prangé,[‖] Ira Katz,[‡] Nathalie Colloc'h[,†]*

† ISTCT UMR 6030 CNRS Univ. Caen Normandie, GIP Cyceron, 14074 Caen, France

‡ Air Liquide Santé International, Innovation Campus Paris, 78354 Les Loges-en-Josas, France

§ UAR 3408 US 50 CNRS INSERM Université de Caen-Normandie, GIP Cyceron, 14074 Caen, France

‖ CiTCoM UMR 8038 CNRS Université de Paris, Faculté de Pharmacie, 75006 Paris, France

Abstract

Argon belongs to the group of chemically inert noble gases, which display a remarkable spectrum of clinically useful biological properties. In an attempt to better understand noble gases, notably argon's mechanism of action, we mined a massive noble gas modelling database which lists all possible noble gas binding sites in the proteins from the Protein Data Bank. We developed a method of analysis to identify amongst all predicted noble gas binding sites, the potentially relevant ones within protein families which are likely to be modulated by Ar. Our method consists in determining within structurally aligned proteins, the conserved binding sites whose shape, localization, hydrophobicity and binding energies are to be further examined. This method was applied to the analysis of two protein families where crystallographic noble gas binding sites have been experimentally determined. Our findings indicate that amongst the most conserved binding sites, either the most hydrophobic one and/or the site which has the best binding energy correspond to the crystallographic noble gas binding sites with the best occupancies, therefore the best affinity for the gas. This method will allow us to predict relevant noble gas binding sites that have potential pharmacological interest and thus potential Ar targets that will be prioritized for further studies including *in vitro* validation.

Introduction

The non-radioactive noble gases, also called the rare or inert gases, belong to the chemical elements in the eighth and last column of the periodic table. This family consists of helium, neon, argon, krypton, and xenon (radon is the radioactive species which is thus not considered). The noble gases are relatively unreactive because they have a complete valence shell, and therefore, have little tendency to gain or lose electrons.

The simplicity of these monoatomic gases and their inertness inclined early biological studies to focus on their physicochemical properties such as solubility in oil or other lipophilic media and blood, and simple biological mechanisms of action such as polar narcosis.[1] They have a remarkably safe clinical profile and readily cross the blood-brain-barrier. Furthermore, they have low solubility in blood, which is advantageous in terms of rapid washin and washout mechanisms.[2] However, the surprising fact is that the noble gases could constitute a new class of therapeutic agents. Numerous studies have identified a rich spectrum of biological effects generated by noble gases that include neuroprotection, tissue protection, reduction of apoptosis, effects on memory, stress and anti-addictive properties.[3] In particular, analgesia and anesthesia induced by xenon, used in humans and animals before comprehensive biochemical studies were conducted[4] have been demonstrated clinically.[5] In spite of the large number of protein targets that noble gases may bind to, only a relatively small number of these targets have been studied and validated to date. Thus, the mechanisms by which the clinically valuable properties are manifest are still ambiguous. In fact, effects on the glutamatergic neurotransmitter systems, especially the N-methyl-D-aspartate (NMDA) receptor, are the most thoroughly studied. It has been shown that xenon's neuroprotective effect may be mediated by inhibition of the NMDA receptor[6] whereas argon also exhibits neuroprotective effects, however, via different mechanisms which remains unclear.[7]

Argon was discovered in 1894.[8] Like the other noble gases, argon is colorless, tasteless, odorless, non-corrosive, non-inflammable, and nontoxic. Because argon is abundant in the atmosphere (0.93 %), thus not really rare and relatively easy to extract from air, especially compared to xenon that is only about 0.9e-5 % in the atmosphere. Therefore, compared to xenon, there would be small production constraints and cost preventing from a large medical usage. Argon mixtures with oxygen for therapeutic use are moderately more dense and viscous than air such that respiratory parameters during ventilation are similar to air.[9] However, this does not preclude the need for devices that are specifically calibrated for argon mixtures. Ventilation with Ar has been shown to be safe both in animals and humans. Indeed, it was reported that ventilation in newborn piglets with up to 80 % argon during normoxia and 50 % argon after hypoxia did not affect heart rate, blood pressure, cerebral saturation and electrocortical brain activity.[10] Another study mentioned that a 6h ventilation with 79 % Ar in pigs showed no toxic effects, as demonstrated by serum biomarkers and assessment of liver and kidney function and structure.[11] Moreover, Lieu and coworkers showed that short treatment with inhaled Ar (50 %) significantly suppressed the microglia/macrophage activation and promoted the M2-like marker arginase 1 at the inner boundary of the infarction seven days after reperfusion in an *in vivo* model of ischemia in rats.[12] More recently, Moro and colleagues found that inhaled Ar (70 %), in traumatic brain injury model, accelerated the recovery of sensorimotor function, induced memory improvements, reduced neuroinflammation in the contused tissue and has anti-oedematous properties.[13] In humans, it has been also reported that the presence of argon in breathing mixtures caused a positive effect on organism adaptation to hypoxia, by examining cardiovascular, pulmonary, nervous systems under normoxic and hypoxic hyperbaric oxygen-nitrogen-argon mixtures.[14]

Preclinical and clinical data support future clinical studies on the role of inhaled Ar as an organ protector. Argon's organoprotective and neuroprotective properties in acute cerebral and myocardial injury, neonatal hypoxic-ischemic encephalopathy, cardiac arrest and organ transplantation have been highlighted in preclinical models in recent years.[15] The description of the potential mechanisms of action involved in Ar protection derives mainly from *in vivo* studies and few cellular *in vitro* assays.[15–20] It has been suggested that argon could have chemical, pharmacological and physical properties similar to those of oxygen, which would explain its neuroprotective effects by partially restoring mitochondrial respiratory enzyme activity and reducing NMDA-induced brain damage.[17] The effects of selective gamma-aminobutyric acid receptor of class A ($GABA_AR$) antagonists on narcosis produced by nitrogen, argon and nitrous oxide have been investigated at high hyperbaric pressure,[21] showing selective antagonism of the narcotic action of nitrogen and argon, but not nitrous oxide. These results suggest that nitrogen and argon could interact directly with the $GABA_A$ receptor.

Moreover, Ar displays anti-apoptotic effects by modulating the molecular pathways involved in cell survival. In particular, *in vitro* models show that Ar increases extracellular signal-regulated kinase ERK1/2 phosphorylation after 30 min of exposure; it blocks the apoptosis cascade; it upregulates the expression of the anti-apoptotic protein B-cell lymphoma-2; it activates the toll-like receptors 2 and 4, which reduce caspase-3 activity, and mediates the intracellular signaling involved in the production of pro-inflammatory cytokines and growth factors.[20] In spite of these studies, there is a need to identify argon's protein targets to better support further research and development as a therapeutic agent.

In structural biology studies, Xe and Kr are useful heavy elements for *de novo* phasing of protein X-ray crystallography data.[22] They can bind to proteins at various types of sites, notably interior,

lipophilic pockets.[23] The crystallographic binding sites of noble gases (Xe, Kr or Ar) are known for around 100 proteins, but the vast majority are only for Xe (i.e.[23–28]). However, such crystallographic experiments to probe the interactions of noble gases with specific proteins are more difficult with gases than with solid or liquid compounds.

In contrast to experiments, the atomic simplicity of the noble gases allows for relatively simple molecular gas-protein docking simulations to be performed such that valuable insights into how they elicit their biological effects may be obtained more quickly and cost-effectively by using *in silico* experiments. It was based on this reasoning that a screening of the five non-radioactive noble gases with approximately 130 000 protein structures in the Protein Data Bank (PDB) was performed. The accuracy of the numerical approach has been validated on existing crystallographic structures of proteins in complex with noble gases.[29] The results of a docking calculations consist of a potential binding energy for all locations around the protein based on a 0.3 Å computational grid. From these thousands of potential binding sites, the 20 most likely, based on their gas binding energy, have been selected for ranking.[30] This noble gas modelling database was developed by a team from Australia's national science agency, the Commonwealth Scientific and Industrial Research Organization (CSIRO), in collaboration with the Air Liquide company.

As a follow up to this previous work,[30] the aim of this paper is to describe the methodology we have employed to extract from this massive noble gas modelling database the protein targets most likely to be involved in biological activity caused by noble gases. We will analyze only results of xenon, krypton and argon binding simulations in our analysis, discarding neon and helium results, since these two gases have lower binding energies so are less likely to generate biological responses.[30]

Described herein is a reorganization of the noble gases interaction database by shared binding sites, an analysis of the shared binding site characteristics, and the methodology to establish a set of five criteria for the characterization of predicted noble gas binding sites which correspond to crystallographic ones. This method of analysis that discriminates relevant noble gas binding sites amongst all predicted ones has been assessed based on the analysis of two protein families. Therefore, this procedure allows the identification of potentially relevant noble gases, notably argon binding sites within protein families which are likely to be modulated by them. This will allow us to predict relevant Ar binding sites that are endowed with potential pharmacological interest and thus Ar targets that will be prioritized for further study including *in-vitro* and *in-vivo* biological validations.

Methods

Data extraction and noble gas modelling database reorganization

For each entry of the noble gas modelling database consisting of the binding site coordinates and binding energies,[30] we retrieved the corresponding Protein Data Bank (PDB) files[31] and added associated noble gas data. For each entry, the 20 best binding sites for each of the noble gases (Xe, Kr, Ar, Ne and He) are ranked by their binding energies, with their binding energies written in the B-factors (temperature factors) column.

We have then reorganized the noble gas modelling database per gas binding sites, building a large spreadsheet, where each line corresponds to a shared gas binding site. An extract of this reorganized database is shown in Figure 1. Two different noble gases are considered to bind in the same site if they are within a distance of 2 Å (average radius of Xe, Kr and Ar). Thereby, a noble

gas binding site is defined by the type of gas that binds, its barycenter, and the neighboring amino-acids, water molecules, other molecules or noble gases that surround it within 5 Å.

id_site	id_pdb	id_Xe	id_Kr	id_Ar	id_He	id_Ne	X	Y	Z	Xe	...	Ne	ALA	...	TYR	HOH	HETATM
1	101m	1	1	1	0	9	26.6	14.576	13.783	0	...	0	1	...	0	2	0
2	101m	2	2	2	14	5	33.331	3.663	5.552	0	...	0	0	...	0	0	1
⋮																	
50	101m	19	0	0	0	0	36.631	-6.987	7.502	0	...	0	0	...	0	1	0

Figure 1. An extract of the spreadsheet containing information on noble gas binding sites. The first column corresponds to the identifier assigned to the site during its extraction, followed by the PDB identifier to which the binding site belongs and the identifiers of noble gases that bind (zero if no binding). X, Y and Z correspond to the spatial coordinates of its barycenter. The following columns are the identifiers of any neighboring noble gases (more than 2 Å and less than 5 Å), the number of each amino-acids types, water molecules and other heteroatoms.

Shared noble gas binding sites characteristics

The binding energy for each gas binding site has been written in the PDB-gas files as previously described. The identifiers for each gas are ranked from 1 to 20 from the strongest to the weakest binding energy. To account for the potential binding across gas species, we defined a new parameter called “rank” that is equal to the average of the Xe, Kr and Ar identifiers for a given binding site. Therefore, this parameter reflects an overall view of the energy profile for a given binding site. The hydrophobicity score of a given binding site corresponds to the number of isoleucine, leucine, valine, phenylalanine, tryptophan, and tyrosine residues divided by the total number of residues that surround the site at less than 5 Å.

Structural alignment of proteins with a selected family

For each analyzed family of proteins, we select several PDB-gas files from various organisms. For PDB entries which have several chains, we split each chain into a single entry. We then structurally align all of them together with their corresponding bound gas. We then discarded non-structurally aligned chains, when the PDB entry corresponds for example, to a hetero-multimer or a complex between different proteins. Therefore, we can readily visualize all the predicted noble gas binding sites within the structurally aligned proteins from the same family.

Spreadsheet generation for a family of proteins

A noble gas binding site is considered to be shared in a family of proteins if the distance between two noble gas atoms in a distinct protein chain is less than 2 Å apart (average radius of Xe, Kr and Ar). Thus, we generate a table that lists, in successive rows, the shared noble gas binding sites in a family. For each shared binding site, we calculated the percentage of conservation for Ar, Kr and Xe, and the average hydrophobicity, rank and binding energy. The resulting spreadsheet was sorted in descending order of Ar conservation and an extract is illustrated in Figure 2.

1fj3_A_gaz_Ar	1fj3_A_gaz_Kr	1fj3_A_gaz_Xe	1gxw_A_gaz_Ar	1gxw_A_gaz_Kr	1gxw_A_gaz_Xe	...	%_Ar	%_Kr	%_Xe	% hydrophobicity	Rank	Ar_energy	Kr_energy	Xe_energy
11	7	8	13	11	10	...	100.00	96.67	83.33	34.44	10.89	-0.914	-1.013	-1.257
6	9	18	4	6	8	...	100.00	100.00	93.33	26.02	5.74	-1.030	-1.116	-1.321
8	14	0	10	15	0	...	96.67	73.33	3.33	27.85	12.50	-0.932	-0.944	-1.144
2	3	6	2	2	3	...	96.67	96.67	96.67	33.33	2.53	-1.094	-1.217	-1.480
13	6	4	12	7	6	...	96.67	96.67	96.67	0.00	7.48	-0.930	-1.086	-1.430
10	8	5	7	5	5	...	96.67	96.67	96.67	64.01	6.06	-0.967	-1.098	-1.434
9	4	2	9	4	2	...	96.67	96.67	96.67	29.39	5.25	-0.948	-1.123	-1.513
1	1	1	1	1	1	...	96.67	96.67	96.67	27.27	1.00	-1.154	-1.318	-1.676
7	11	0	6	9	15	...	96.67	86.67	26.67	32.01	10.76	-0.945	-0.976	-1.166
.	.	.	.	.	.	.	.	.	.	.	.	.	.	.
.	.	.	.	.	.	.	.	.	.	.	.	.	.	.
.	.	.	.	.	.	.	.	.	.	.	.	.	.	.

Figure 2. An extract of the generated spreadsheet containing information on shared noble gas binding sites within the thermolysin family. In each row, the identifiers for the three gases are

given (0 if no gas bound), followed by the percentage of conservation of Ar, Kr and Xe, the average hydrophobicity, rank and binding energies.

Analysis procedure for a family of proteins

We first select a large set of proteins from the family we would like to analyze. To avoid possible bias with crystallographic structures pressurized with noble gases, we discarded them from our analysis. We then build the spreadsheet listing all shared binding sites as described above. We will then analyze further the ten or so most conserved binding sites, choosing a threshold which depends on the variety of species in the protein family. For example, if the available PDB entries for a family belong to the same species and correspond to a unique gene, the chosen threshold will be high. On the other hand, if the available PDB entries correspond to many different genes across species, the chosen threshold will be lower. The predicted binding sites were either located too close to the atoms of the protein or were not associated to well-defined cavities, these sites were discarded from our analysis. To validate this procedure, we applied it to the crystallographic structures of two interesting protein families, thermolysin (a member of metallo-proteinases) and neuroglobin (a member of the globin family) whose noble gases binding sites have been experimentally determined.

Software

We generated PDB-gas files in PDB format using the BioPython library which is a set of freely available tools for biological computation written in Python, allowing efficient and simplified manipulation of PDB files.

We developed Python 3.6.5 scripts to reorganize the noble gas modelling database and to characterize the noble gas binding sites.

The structural alignment of a family of proteins with their associated predicted noble gas binding sites were performed using the "Align" command from PyMol software (The PyMOL Molecular Graphics System, Version 2.4.0 Schrödinger, LLC), based on a sequence alignment. We calculated distances between noble gas atoms within all the aligned structures to determine the ones which share the same positions, using SciPy (https://www.scipy.org/) package which is a collection of mathematical algorithms and convenience functions built on the NumPy (https://numpy.org/) extension of Python. We then calculated for each binding site the percentage of conservation of the three noble gases (Ar, Kr and Xe), its rank and its average hydrophobicity and gas binding energies using Pandas toolkit. Pandas is open source data analysis and manipulation toolkit, built on top of the Python programming language.

Results

Shared noble gas binding sites characterization

A general characterization of the computationally predicted noble gas binding sites listed in the noble gas modelling database was performed separately for each noble gas type, by analyzing their binding energies, their environments and their proximities to residues and to natural ligand.[30] In this work, we have analyzed the same database however using a different approach, investigating and characterizing the binding sites shared between different noble gas. To be able to perform this analysis, we reorganized the noble gas modelling database per binding sites. We have first retrieved almost 128 000 PDB-gas entries with 20*5 noble gas binding sites (see the Methods section). We then built the reorganized database by binding sites instead of gas types, which consists of a large spreadsheet listing the almost 6.8 M noble gas binding sites and their neighbors.

There are on average 53 ± 7 shared binding sites per PDB-gas entry and about 7 ± 1 amino-acids surrounding each shared binding site.

Our analysis of the shared binding sites revealed that almost half of the sites bind only Ne and/or He. Of the remaining sites, about 15 % bind Xe and Kr, but not Ar, and 8 % bind Ar but not Xe or Kr.

The shared binding site hydrophobicity has been also analyzed, with a distribution of the residues in six classes from the most hydrophobic to the least ones according to the hydrophobicity scoring matrix constructed from hydrophilicity data.[32,33] The hydrophobicity of sites is inversely proportional to the noble gas atom's diameter, as described in Figure 3, the smaller the atom, the more hydrophobic is the binding site. These properties of noble gases binding sites are also verified when they were previously analyzed according to their gas types.[30]

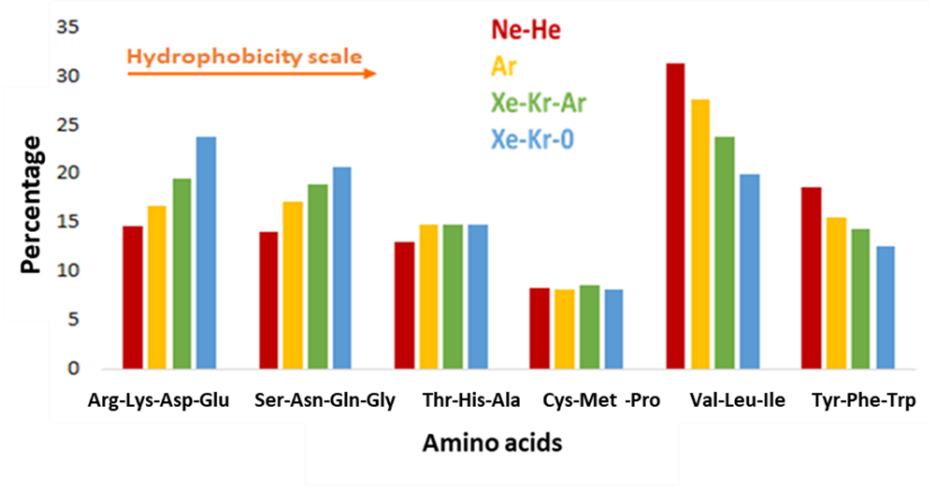

Figure 3. Percentage of amino acids grouped together in six classes surrounding noble gas binding sites. Red bars represent He and/or Ne specific binding sites, yellow bars represent Ar but not Xe and Kr binding sites, green bars represent Xe, Kr and Ar binding sites and blue bars represent Xe and Kr but not Ar binding sites.

In the noble gas modelling database, as previously calculated,[30] average binding energy for Xe (-1.246 ± 0.203 kcal/mol) is higher than for Kr (-0.991 ± 0.154 kcal/mol), itself higher than for Ar (-0.902 ± 0.131 kcal/mol), as expected in the order of their polarizabilities.[34] It was noted that noble gas binding energies need to be relatively stronger in absolute magnitude than the thermal energy at RT (~0.6 kcal/mol at 37 °C) at physiological conditions to induce potentially biological effects on proteins.[30]

Characterization of conserved gas binding sites within a family of proteins

Our method of analysis of the reorganized database allows the extraction of putative interesting targets for Ar, based on a series of criteria to identify potentially relevant binding sites, such as the conservation of a binding site across a family, its localization and its physical-chemical characteristics (see the Methods section). If a binding site is physiologically relevant, it should be conserved within a given family of proteins synthesized by different species. Herein, we structurally aligned selected protein structures from a family to be able to identify shared noble gas binding sites within the family, that are stored in a spreadsheet. The most conserved binding sites within the family, above a given threshold, which will depend on the variations in sequence in the analyzed family, will be more thoroughly analyzed.

For each binding site an average hydrophobicity, an average binding energy per noble gas, and an average rank that gives a global estimate of the binding energy for the three gases are calculated. Relevant binding sites are expected to be hydrophobic, since noble gases bind preferably to hydrophobic pockets and cavities.[23,35] Moreover, noble gases should bind with a high energy in the relevant binding sites.

Comparison between crystallographic binding sites and conserved binding sites in two families of proteins

Two families of proteins, thermolysin and neuroglobin have been chosen to asses our selection of relevant binding sites amongst the 20 best ones identified in the modelling database. Their crystallographic Xe, Kr and Ar binding sites are precisely known, and their main binding sites are located in functional areas, suggesting that a bound noble gas would induce functional modification. Crystallographic structures under pressurized noble gas give access to the coordinates of the gas and to its occupancy which is an estimate of its affinity for this site and follows a pressure-response curve, increasing with the applied gas pressure up to a plateau.[24]

Thermolysin family analysis

In the structure of *Bacillus thermoproteolyticus* thermolysin (TLN), Xe [36] and Kr [37] bind with a high occupancy (81 % Xe at 3.5 MPa, 69 % Kr at 4 MPa), to a binding site located in a cavity (termed here gas binding site 1 or GBS1) (Table 1).

This cavity, also termed reference cavity 2[36] is surrounded by the side chains of Tyr^{84}, Ser^{92}, Leu^{144} and Val^{148}. Kr binds also to a second site, termed here GBS2, with a lower occupancy (25 % Kr at 4 MPa). This site corresponds to a small cavity, located at 7.2 Å from the first one, surrounded by Arg^{35}, Gly^{36}, Asn^{37}, Gly^{38} and Asn^{97}. Ar binds at 200 MPa with a full occupancy in these two cavities (P. Carpentier and T. Prangé, private communication, PDB ID *6qar*). Both cavities are likely to be allosteric since they are close to the TLN catalytic center around the zinc binding site as shown in Figure 4.

Table 1. The crystallographic noble gas binding sites within TLN structures

Noble gas		Xe		Kr			Ar
PDB ID		*5m69*	*3ls7*	*5m5f*	*5fss*	*5fsp*	*6qar*
Pressure (MPa)		0.9	3.5	0.5	4	10	200
Occupancy (%)	**GBS1**	68	81	20	69	100	100
	GBS2	0	0	0	25	55	100

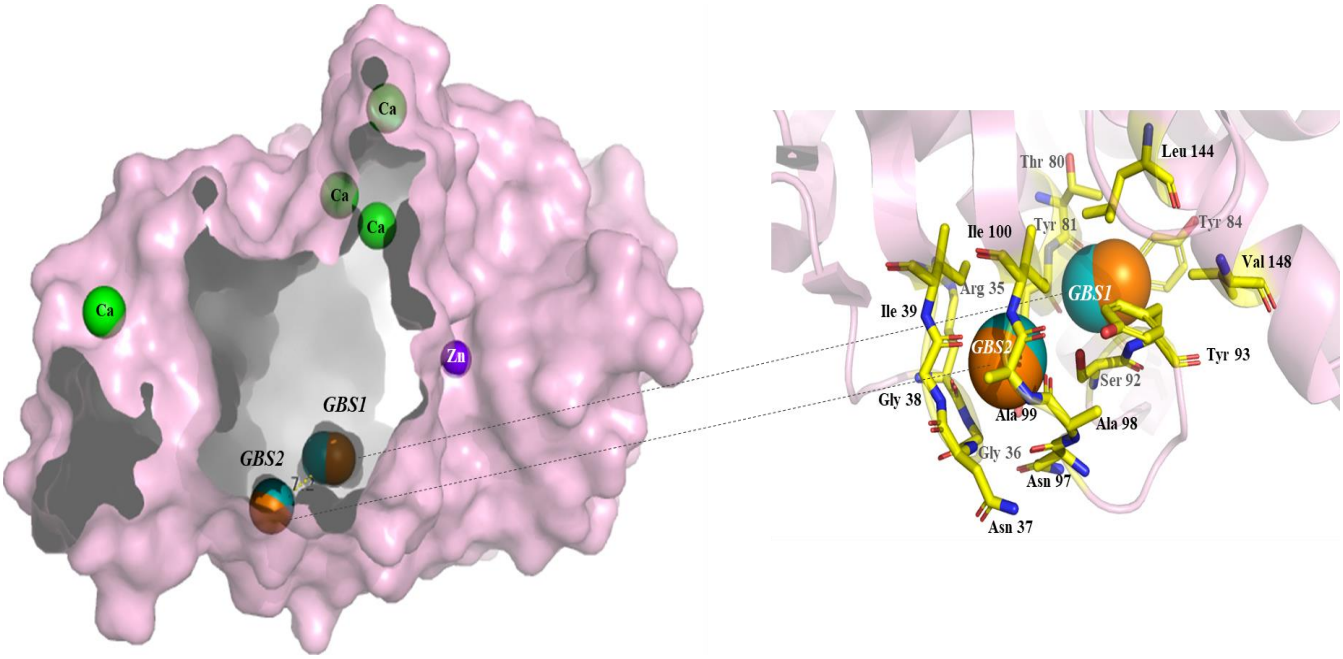

Figure 4. Visualization of the two major crystallographic noble gas binding sites shown as orange spheres in TLN structure (PDB ID *5fss*), and their corresponding predicted binding sites shown as cyan spheres. TLN is shown with its molecular surface, with calcium and zinc ions as spheres. Residues surrounding GBS1 and GBS2 are shown in stick representation in the zoomed view.

We superimposed 29 TLN crystallographic structures extracted from the noble gas modelling database, split into 30 chains, all derived from *Bacillus thermoproteolyticus*. The resulting nine most conserved binding sites are listed in Table 2, using a high threshold of 90 % of conservation due to the unique specie in the family, after removal of sites without any volumes.

The binding site #3 is located at less than 1.1 Å from the main crystallographic binding sites GBS1, and the binding site #5 is located at less than 1 Å from GBS2. Interestingly, amongst the nine most conserved sites, the most hydrophobic one corresponds to GBS1 and the site which has the strongest (i.e., the most negative) binding energy (the lower rank) correspond to GBS2.

Table 2. The most conserved predicted noble gas binding sites within TLN structures

Site identifier	**% Ar**	**% Kr**	**% Xe**	**% Hydrophobicity**	**Rank**	**Ar energy (kcal/mol)**	**Kr energy (kcal/mol)**	**Xe energy (kcal/mol)**
1	100.00	96.67	83.33	34.44	10.89	-0.914	-1.013	-1.257
2	96.67	96.67	96.67	0.00	7.48	-0.930	-1.086	-1.430
3	**96.67**	**96.67**	**96.67**	**64.01**	**6.06**	**-0.967**	**-1.098**	**-1.434**
4	96.67	96.67	96.67	29.39	5.25	-0.948	-1.123	-1.513
5	**96.67**	**96.67**	**96.67**	**27.27**	**1.00**	**-1.154**	**-1.318**	**-1.676**
6	96.67	96.67	96.67	0.00	3.92	-1.027	-1.150	-1.446
7	96.67	73.33	3.33	27.85	12.50	-0.932	-0.944	-1.144
8	53.33	93.33	86.67	38.46	11.83	-0.853	-0.971	-1.253
9	50.00	90.00	86.67	54.23	14.29	-0.847	-0.949	-1.182

Neuroglobin family analysis

In the structure of murine neuroglobin (NGB), Xe, Kr and Ar bind with high occupancies in two sites as shown in Table 3, the storage site (90 % Xe at 3 MPa, 60 % Kr at 5 MPa and 30 % Ar at 5 MPa) and the BD-pocket (55 % Xe at 3 MPa and 30 % Kr at 5 MPa).[27,35,38] Ar is visible in the B-D pocket only at 200 MPa (P. Carpentier and T. Prangé private communication, PDB ID *6r1q*). The storage site is located in the large internal heme cavity which plays a key role in the ligand binding mode through its structural flexibility and plasticity and constitutes the dioxygen storage site before it reacts with the Fe-bound heme.[39] This site has a high affinity for Xe and Ar since both gases bind at a moderate gas pressure (Table 3). Since it was experimentally shown that the dioxygen molecule is bound in this site before being bound to the heme, we infer that a noble gas bound in this site could modulate neuroglobin activity. This site is lined by the hydrophobic residues Ile,[72] Leu[113], Trp[133], Tyr[137], Leu[136] and Val[140] as described in Figure 5. The B-D pocket is situated in a solvent-accessible surface pocket between helices B and D. It is slightly less hydrophobic than the storage site and flanked by two polar residues Thr[25] and Ser[55].

Table 3. The crystallographic noble gas binding sites within NGB structures

Noble gas		**Xe**					**Kr**				**Ar**	
PDB ID		*3gk9*	*3gln*	*5o1k*	*4o4t*	*5o27*	*3gkt*	*5nw6*	*5o17*	*6eye*	*5nvi*	*6r1q*
Pressure (MPa)		2	2	2	3	3	4	5	10	15	5	200
Occupancy	**Storage site**	80	75	90	90	90	47	60	100	30	30	100
(%)	**B-D pocket**	48	40	40	55	70	32	30	80	100	0	100

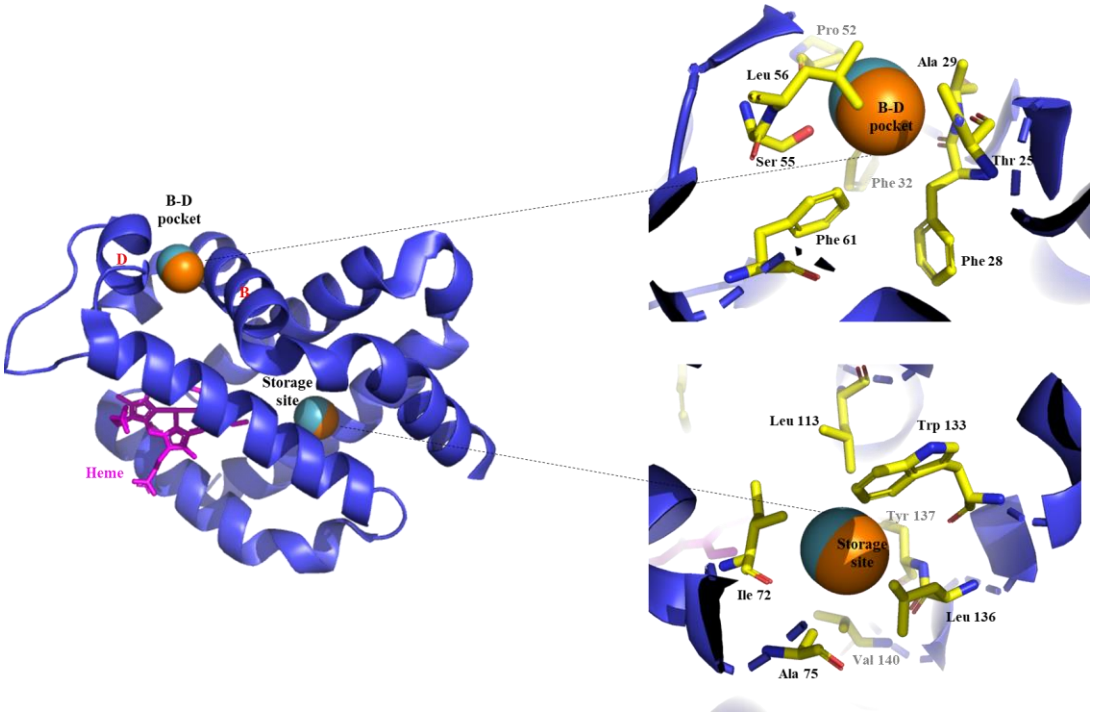

Figure 5. Visualization of the two major crystallographic noble gas binding sites shown as orange spheres in NGB structure (PDB ID *5o17*), and their corresponding predicted binding sites shown as cyan spheres. NGB is shown as cartoon representation, with the heme as sticks. Residues surrounding the B-D pocket and the storage site are shown in stick representation in the two inserts.

We superimposed 17 NGB crystallographic structures extracted from the noble gas modelling database, split into 21 chains, from three species, *Homo sapiens, Mus musculus* and *Symsagittifera roscoffensis*. We ended up with the nine most conserved binding sites, using a threshold of 70 % of conservation, that are listed in Table 4, after removal of sites without any volumes.

The binding site #5 is located at less than 0.5 Å from the storage site, and the binding site #8 is located at less than 0.8 Å from the B-D pocket site. Here also, amongst the nine most conserved sites, the most hydrophobic one and the site that has the best binding energy for the three noble gases (the lowest rank) correspond to the two major crystallographic binding sites, respectively.

Table 4. The most conserved predicted noble gas binding sites within NGB structures

Site identifier	% Ar	% Kr	% Xe	% Hydrophobicity	Rank	Ar energy (kcal/mol)	Kr energy (kcal/mol)	Xe energy (kcal/mol)
1	85.71	90.48	61.90	65.66	6.92	-0.917	-0.965	-1.123
2	80.95	80.95	76.19	62.32	8.00	-0.870	-0.942	-1.164
3	76.19	76.19	76.19	48.04	5.58	-0.900	-0.964	-1.182
4	76.19	76.19	76.19	35.57	6.79	-0.846	-0.957	-1.236
5	**71.43**	**90.48**	**95.24**	**87.74**	**5.19**	**-0.877**	**-1.003**	**-1.280**
6	71.43	76.19	66.67	22.50	12.76	-0.784	-0.870	-1.075
7	71.43	71.43	38.10	37.08	12.61	-0.824	-0.862	-1.046
8	**66.67**	**71.43**	**76.19**	**50.45**	**4.00**	**-0.892**	**-0.997**	**-1.242**
9	61.90	71.43	66.67	49.07	9.71	-0.806	-0.912	-1.167

Discussion

In a previous paper the *in silico* results of noble gas-protein binding sites were characterized in a global sense.[30] In that previous paper the fundamental tendencies of the binding sites were characterized, according to each noble gas type, with their binding energy; their overall hydrophobicity; their proximity to natural ligands; and proximity to residues within the binding pocket.

In this paper, a method is presented to choose amongst all predicted noble gas binding sites, the potentially relevant ones within protein families which are likely to be modulated by Ar. A preliminary reorganization of the noble gas modelling database per shared binding sites were needed to consider simultaneously the heavier noble gas binding sites (Xe, Kr, Ar) in our analysis. Our method consists in determining within structurally aligned proteins, the conserved binding sites whose shape, localization, hydrophobicity and binding energies are likely to result in Ar bioactivity. Our reasoning is grounded on the fact that, experimentally, we detect only a couple of crystallographic binding sites with high occupancies, i.e. high affinity, within crystallized proteins under pressurized noble gases. Therefore, there is an obvious need to follow up the previous work by pointing out reliably the most relevant noble gas binding sites which are likely to modulate the protein function in order to spot potential targets for argon that will be prioritized for crystallographic and biological validations.

Our procedure is mainly based on the conservation of the noble gas binding sites within a structurally aligned protein family. We found that the main crystallographic noble gas binding site in TLN and NGB corresponds to the most hydrophobic one amongst the most conserved sites, confirming that noble gases have a preference to bind to hydrophobic cavities, accessible or buried in the core structure of the protein.[23] However, in both families, the second crystallographic noble gas binding site corresponds to a site which is less hydrophobic, but which binds the gas with the highest binding energy. Our method seems thus to be efficient to identify amongst the predicted noble gas binding sites the ones that are likely to be physiologically relevant, corresponding to experimentally determined ones, where the gas bind with a high occupancy, i.e. a high affinity. Therefore, our hypothesis regarding the conservation of an interesting noble gas binding site within a structurally aligned protein family seems pertinent since it has been verified in both analyzed

protein families. Of course, the conservation criterion is more efficient for a large family that extends over many genes and species than for a family where all the determined crystallographic structures correspond to a unique gene as it is the case for TLN.

In protein-ligand interactions, usually a few key residues are involved, defining the functional site in a given protein. Pharmaceutical compounds are designed to bolster or inhibit its biological function. If a noble gas binding at a given site induces a modulation of the function of a protein, it should be located close to a region that is involved in its activity such as an active site, an allosteric site or a surface involved in interaction with partners. In both TLN and NGB analyzed families, the noble gases bind to sites which are likely to modulate the protein activity, especially in NGB where noble gases bind in the dioxygen storage site.

Thus, we have defined a set of five criteria to detected relevant gas binding sites amongst all predicted ones which are the conservation of a binding site across a protein family, its physical-chemical characteristics defined by its binding energy, its hydrophobicity and its associated volume and obviously its localization within a region involved in the protein activity modulation. If the analysis of a given family of a protein provides no predicted sites that satisfy the five criteria, we suggest that this family would not constitute a potential target for Ar. Conversely, if one or more potentially interesting binding sites are detected in our analysis, we hypothesize that argon could modulate the activity of this family, opening the way to further *in vitro* validation.

The rate of conservation of a binding site for a gas across a family could not reflect the relative occupancy of the three gases. In NGB, whose family spans various species, the rate of conservation for Xe is higher than for Ar in the two main crystallographic sites, even if the three gases are experimentally found to bind in both sites. In TLN whose structures correspond to a unique gene, the three gases are predicted to bind to the two major sites with the same rate of conservation

across the family. However, GBS2 seems to be an Ar and Kr specific site, where Xe cannot bind, perhaps because of the small size of the pocket. This specificity for Ar and Kr could not be found with our method of analysis. Noble gases, notably Xe and Ar, are known, not only, to exhibit different biological effects but also to be target-specific.[7,40] It is possible that our method of analysis which highlights only the most conserved sites could miss a less conserved one, which would be specific for a given gas.

Although noble gases are described as inert, they are biologically active, with the heaviest ones having been shown to be the most active. However, the mechanisms of action of this activity are still unclear. The lighter noble gases helium and neon exert little effect on biological processes. They are not anesthetics, nor analgesics. He has a high thermal conductivity, and heat loss from the body may occur when it is completely immersed in helium.[41] In rats, extended breathing of 75 % He resulted in significantly reduced brain infarct size and improved functional neurological outcome.[42] The authors conclude that the neuroprotective effects of helium are due to hypothermia rather than to a pharmacological effect. Neon, based on its oil solubility, is predicted to be an anesthetic at ~160 atm.[5] But it is unlikely to have a pharmacological neuroprotective effect at atmospheric pressures. He and Ne appear both chemically and biologically inactive.

Accordingly, our global analysis of predicted He and Ne binding sites in the noble gas modelling database revealed that more than half of their binding sites are specific and not shared with the heavier noble gases binding sites. Moreover, the modelled binding sites where only Xe and/or Kr bind are not shared with Ar, Ne and He. He and Ne are likely to bind to a variety of sites without biological relevance.

Noble gases preferentially bind to hydrophobic cavities or pockets.[23] However, when we analyzed more thoroughly the amino-acids that are in close proximity to the modelled gases (less than 5 Å),

we noticed that while the He and Ne show affinity to highly hydrophobic environment (more than 50 % of hydrophobic residues), Xe and Kr tend to prefer less hydrophobic ones (only 32 % of hydrophobic residues), with Ar binding sites lying between them (43 % hydrophobic residues). Even if noble gases are considered as inert, they interact with their environment through three weak-energy attractive forces: charge-induced, dipole-induced, and London (also called dispersion) interactions. In fact, while induced dipole interactions occur only when the noble gas atom is located in the proximity of charged or polar protein groups, London interactions rule the majority of both polar and nonpolar binding sites.[22] These interactions are proportional to the electronic polarizability of the noble gas atom, i.e. its number of electrons. The heavier the noble gas is, the more polarizable it is (Table 5), which would explain the presence of charged residues around the heavier noble gases. The crystallographic occupancies of noble gases within a given binding site at a given pressure are indeed in the order of their electronic polarizabilities.[28,34] It is verified in TLN and NGB, where Xe occupancy is higher than Kr occupancy, itself higher than Ar occupancy for a given binding site at a given pressure (Tables 1 and 3). Experimentally, the pressure that allows to populate a gas binding site is obviously in the reverse order than the polarizabilities, rather low for Xe (~ 0.5 - 3 MPa), moderate for Kr (~ 1 - 20 MPa), and higher for Ar (~ 50 - 200 MPa) which could be located at 50 MPa only in very affine sites.

Table 5. Van der Waals radii and polarizabilities of non-radioactive noble gases (taken from[34]) and their natural abundance in air (taken from[43])

Noble gas	Atomic number	Van der Waals radius (Å)	Polarizability (Å^3)	Dry air abundance (ppmv[a])
He	2	1.40	0.20	5.2

Ne	10	1.54	0.40	18,2
Ar	18	1.91	1.64	9340
Kr	36	2.03	2.48	1.1
Xe	54	2.21	4.04	0.09

[a] ppmv parts per million by volume fraction ≈ parts per million by mole fraction.

Even though the docking study used to construct the noble gas modelling database was performed with static target crystal structures and rigid noble gases without any consideration of their electronic polarizabilities,[30] it nonetheless succeeded at predicting more polar noble gas binding sites stabilized through their electronic polarizability. However, the rigid sphere procedure of docking obviously does not take into account the thermal fluctuations that foster exploration of the multiple and complex conformational substates with different shapes of binding sites within proteins. For example, in an early docking study[44], molecular dynamics (MD) simulations have highlighted the existence of a large number of thermally accessible minima in myoglobin, which have an essential role in determining the protein internal motions. Simulations of noble gases with proteins were performed first by Tilton and co-workers[45] to investigate further the interaction of Xe with myoglobin. By calculating empirical energy, they found that van der Waals' interactions are mainly responsible for Xe binding with smaller contributions of Xe polarization. Along the same lines, Hermans and Shankar[46] calculated the free energy of xenon binding to myoglobin by applying MD with forcing potential. They found that the insertion of the first xenon atom causes a perturbation of the protein conformation that facilitated the binding of additional xenon atoms. Very good agreement was obtained between theoretically and experimentally determined affinities. The complexes of phage T4 lysozyme L99A, has been studied by MD simulation in

presence of Xe, Kr and Ar.[47] The binding positions and the calculated affinities agree closely with the positions of bound Xe determined in the refined crystal structure of a complex formed at a pressure of 8 bar Xe and with the observed partial occupancies respectively. Xenon was found to have favorable characteristics for binding due to its large atomic polarizability, its application at a relatively high pressure and its rotational independence. In another study, Liu and coworkers performed several MD simulations on the open and closed cleft ligand-binding domains (LBDs) of the NMDA receptor with and without the Xe atom and they have identified potential Xe binding sites nearby agonist sites, in the hinge region, and at the interface between two subunits.[48] However, it is noteworthy that MD are computationally expensive methods for more than a few proteins, thus, we have thoroughly analyzed the previously elaborated massive noble gas modelling database[30] to filter out potentially relevant Ar protein targets. Interestingly, our applied method turns out to be efficient to accurately determine relevant noble gas binding sites within protein families.

Conclusion

In this work, we proposed a set of five criteria to identify relevant noble gas binding sites in potentially interesting protein targets. These sites have been carefully selected from the reorganized database containing the predicted noble gas binding sites that have been previously generated as described in the former study led by Winkler et al.[30], using our criteria for being the more likely ones to induce a biological effect in the analyzed protein family. Different protein families whose crystallographic binding sites are unknown have been analyzed by applying our procedure. We have already identified potentially relevant gas binding sites which are conserved across protein families and following our set of criteria (hydrophobicity, gas binding energy,

localization). Several potential targets have emerged from our analysis; for example, nitric oxide synthase, guanylate cyclase or metabotropic glutamate receptors where one or two potentially relevant gas binding sites have been identified. Biological validation plans are currently being considered for these proteins, and therefore we anticipate that we will be able to formulate new hypotheses about the mechanism of action of argon.

Interestingly, our analysis has also returned negative conclusions for several studied families. For example, we found no putative relevant noble gas binding sites among the predicted ones in E2 and E3 ligases, the β-subunits of voltage gated potassium channels and high-temperature requirement A serine proteases. Although we found in these families several conserved binding sites which might partially satisfy our suggested criteria, their localization suggest that they would rather correspond to non-specific binding sites into pre-existing non-functional cavities, thus inducing no functional modification. Indeed, it is known that noble gases bind to specific sites in a definite number of proteins to elicit their biological effect. These results suggest that our method of analysis is relevant, in that it does not find interesting binding sites in all families of proteins.

AUTHOR INFORMATION

Corresponding Author

Nathalie Colloc'h - ISTCT UMR 6030 CNRS Univ. Caen Normandie, GIP Cyceron, 14074 Caen, France. ORCID iD: 0000-0002-2764-6026

Email: colloch@cyceron.fr

Authors

Islem Hammami - ISTCT UMR 6030 CNRS Univ. Caen Normandie, GIP Cyceron, 14074 Caen, France, Air Liquide Santé International, Innovation Campus Paris, Les Loges-en-Josas, France

Géraldine Farjot - Air Liquide Santé International, Innovation Campus Paris, 78354 Les Loges-en-Josas, France. ORCID iD: 0000-0003-0945-6365

Mikaël Naveau - UAR 3408 US 50 CNRS INSERM Université de Caen-Normandie, GIP Cyceron, 14074 Caen, France. ORCID iD: 0000-0002-4685-0057

Audrey Rousseaud - Air Liquide Santé International, Innovation Campus Paris, 78354 Les Loges-en-Josas, France. ORCID iD: 0000-0002-5617-2501

Thierry Prangé - CiTCoM UMR 8038 CNRS Université de Paris, Faculté de Pharmacie, 75006 Paris, France. ORCID iD: 0000-0002-7129-7396

Ira Katz - Air Liquide Santé International, Innovation Campus Paris, 78354 Les Loges-en-Josas, France. ORCID iD: 0000-0001-6755-9739

Notes

The authors declare no competing financial interest.

Acknowledgements

Islem Hammami was supported by the CIFRE Grant 2019/0919 from the "ANRT" (National Association for Research and Technology). The study was supported by Air Liquide Santé International.

Data and Software Availability

The noble gas modelling database is freely available in compressed form in data archives at La Trobe University OPAL/Figshare (DOI: 10.26181/617b2977824d2).

Protein Data Bank (https://www.rcsb.org) was used for uploading protein 3D structures.

PYMOL (The PyMOL Molecular Graphics System, Version 2.4.0 Schrödinger, LLC) (https://pymol.org) was used for noble gases and protein structures visualization.

The different tools developed and described in this paper are written in python programming language and are available on demand.

ABBREVIATIONS

PDB, Protein Data Bank; CSIRO, Commonwealth Scientific and Industrial Research Organization; NMDA, N-methyl-D-aspartate; TLN, Thermolysin; NGB, Neuroglobin; GBS, Gas Binding Site; MD, molecular dynamics.

REFERENCES

(1) Yeh, S.-Y.; Peterson, R. E. Solubility of Krypton and Xenon in Blood, Protein Solutions, and Tissue Homogenates. *J. Appl. Physiol.* **1965**, *20*, 1041–1047. https://doi.org/10.1152/jappl.1965.20.5.1041.

(2) Harris, P. D.; Barnes, R. The Uses of Helium and Xenon in Current Clinical Practice. *Anaesthesia* **2008**, *63*, 284–293. https://doi.org/10.1111/j.1365-2044.2007.05253.x.

(3) Winkler, D. A.; Thornton, A.; Farjot, G.; Katz, I. The Diverse Biological Properties of the Chemically Inert Noble Gases. *Pharmacol. Ther.* **2016**, *160*, 44–64. https://doi.org/10.1016/j.pharmthera.2016.02.002.

(4) Cullen, S. C.; Gross, E. G. The Anesthetic Properties of Xenon in Animals and Human Beings, with Additional Observations on Krypton. *Science* **1951**, *113*, 580–582. https://doi.org/10.1126/science.113.2942.580.

(5) Dickinson, R.; Franks, N. P. Bench-to-Bedside Review: Molecular Pharmacology and Clinical Use of Inert Gases in Anesthesia and Neuroprotection. *Crit. Care* **2010**, *14*, 229. https://doi.org/10.1186/cc9051.

(6) Franks, N. P.; Dickinson, R.; de Sousa, S. L. M.; Hall, A. C.; Lieb, W. R. How Does Xenon Produce Anaesthesia? *Nature* **1998**, *396*, 324–324. https://doi.org/10.1038/24525.

(7) Koziakova, M.; Harris, K.; Edge, C. J.; Franks, N. P.; White, I. L.; Dickinson, R. Noble Gas Neuroprotection: Xenon and Argon Protect against Hypoxic–Ischaemic Injury in Rat Hippocampus in Vitro via Distinct Mechanisms. *Br. J. Anaesth.* **2019**, *123*, 601–609. https://doi.org/10.1016/j.bja.2019.07.010.

(8) Rayleigh, Lord; Ramsay, W. Argon, a New Constituent of the Atmosphere. *Philos. Trans. R. Soc. Lond. A* **1895**, *186*, 187–241.

(9) Katz, I.; Milet, A.; Chalopin, M.; Farjot, G. Numerical Analysis of Mechanical Ventilation Using High Concentration Medical Gas Mixtures in Newborns. *Med. Gas Res.* **2019**, *9*, 213–220. https://doi.org/10.4103/2045-9912.273959.

(10) Alderliesten, T.; Favie, L. M. A.; Neijzen, R. W.; Auwärter, V.; Nijboer, C. H. A.; Marges, R. E. J.; Rademaker, C. M. A.; Kempf, J.; van Bel, F.; Groenendaal, F. Neuroprotection by Argon Ventilation after Perinatal Asphyxia: A Safety Study in Newborn Piglets. *PLoS One* **2014**, *9*, e113575. https://doi.org/10.1371/journal.pone.0113575.

(11) Martens, A.; Ordies, S.; Vanaudenaerde, B.; Verleden, S.; Vos, R.; Verleden, G.; Verbeken, E.; Van Raemdonck, D.; Claes, S.; Schols, D.; Chalopin, M.; Katz, I.; Farjot, G.; Neyrinck, A. A Porcine Ex Vivo Lung Perfusion Model with Maximal Argon Exposure to Attenuate Ischemia-Reperfusion Injury. *Med. Gas Res.* **2017**, *7*, 28. https://doi.org/10.4103/2045-9912.202907.

(12) Liu, J.; Nolte, K.; Brook, G.; Liebenstund, L.; Weinandy, A.; Höllig, A.; Veldeman, M.; Willuweit, A.; Langen, K.-J.; Rossaint, R.; Coburn, M. Post-Stroke Treatment with Argon Attenuated Brain Injury, Reduced Brain Inflammation and Enhanced M2 Microglia/Macrophage Polarization: A Randomized Controlled Animal Study. *Crit. Care* **2019**, *23*, 198. https://doi.org/10.1186/s13054-019-2493-7.

(13) Moro, F.; Fossi, F.; Magliocca, A.; Pascente, R.; Sammali, E.; Baldini, F.; Tolomeo, D.; Micotti, E.; Citerio, G.; Stocchetti, N.; Fumagalli, F.; Magnoni, S.; Latini, R.; Ristagno, G.; Zanier,

E. R. Efficacy of Acute Administration of Inhaled Argon on Traumatic Brain Injury in Mice. *Br. J. Anaesth.* **2021**, *126*, 256–264. https://doi.org/10.1016/j.bja.2020.08.027.

(14) Pavlov, B. N.; Buravkov, S. V.; Soldatov, P. E.; Vdovin, A. V.; Deviatova, N. V. The Effects of Oxygen-Argon Gaseous Mixtures on Humans Under Long-Term Hyperbaric Condition. In *Advances in High Pressure Bioscience and Biotechnology*; Springer: Berlin, Heidelberg, 1999; pp 561–564.

(15) Nespoli, F.; Redaelli, S.; Ruggeri, L.; Fumagalli, F.; Olivari, D.; Ristagno, G. A Complete Review of Preclinical and Clinical Uses of the Noble Gas Argon: Evidence of Safety and Protection. *Ann. Card. Anaesth.* **2019**, *22*, 122. https://doi.org/10.4103/aca.ACA_111_18.

(16) Broad, K. D.; Fierens, I.; Fleiss, B.; Rocha-Ferreira, E.; Ezzati, M.; Hassell, J.; Alonso-Alconada, D.; Bainbridge, A.; Kawano, G.; Ma, D.; Tachtsidis, I.; Gressens, P.; Golay, X.; Sanders, R. D.; Robertson, N. J. Inhaled 45–50% Argon Augments Hypothermic Brain Protection in a Piglet Model of Perinatal Asphyxia. *Neurobiol. Dis.* **2016**, *87*, 29–38. https://doi.org/10.1016/j.nbd.2015.12.001.

(17) David, H. N.; Haelewyn, B.; Degoulet, M.; Colomb, D. G.; Risso, J.-J.; Abraini, J. H. Ex Vivo and In Vivo Neuroprotection Induced by Argon When Given after an Excitotoxic or Ischemic Insult. *PLoS One* **2012**, *7*, e30934. https://doi.org/10.1371/journal.pone.0030934.

(18) Gardner, A. J.; Menon, D. K. Moving to Human Trials for Argon Neuroprotection in Neurological Injury: A Narrative Review. *Br. J. Anaesth.* **2018**, *120*, 453–468. https://doi.org/10.1016/j.bja.2017.10.017.

(19) Lemoine, S.; Blanchart, K.; Souplis, M.; Lemaitre, A.; Legallois, D.; Coulbault, L.; Simard, C.; Allouche, S.; Abraini, J. H.; Hanouz, J.-L.; Rouet, R.; Sallé, L.; Guinamard, R.; Manrique, A. Argon Exposure Induces Postconditioning in Myocardial Ischemia–Reperfusion. *J. Cardiovasc. Pharmacol. Ther.* **2017**, *22*, 564–573. https://doi.org/10.1177/1074248417702891.

(20) Ulbrich, F.; Goebel, U. The Molecular Pathway of Argon-Mediated Neuroprotection. *Int. J. Mol. Sci.* **2016**, *17*, 1816. https://doi.org/10.3390/ijms17111816.

(21) Abraini, J. H.; Kriem, B.; Balon, N.; Rostain, J.-C.; Risso, J.-J. Gamma-Aminobutyric Acid Neuropharmacological Investigations on Narcosis Produced by Nitrogen, Argon, or Nitrous Oxide. *Anesth. Analg.* **2003**, *96*, 746–749, table of contents. https://doi.org/10.1213/01.ane.0000050282.14291.38.

(22) Schiltz, M.; Fourme, R.; Prangé, T. Use of Noble Gases Xenon and Krypton as Heavy Atoms in Protein Structure Determination. *Methods Enzymol.* **2003**, *374*, 83–119. https://doi.org/10.1016/S0076-6879(03)74004-X.

(23) Prangé, T.; Schiltz, M.; Pernot, L.; Colloc'h, N.; Longhi, S.; Bourguet, W.; Fourme, R. Exploring Hydrophobic Sites in Proteins with Xenon or Krypton. *Proteins Struct. Funct. Bioinforma.* **1998**, *30*, 61–73. https://doi.org/10.1002/(SICI)1097-0134(19980101)30:1<61::AID-PROT6>3.0.CO;2-N.

(24) Marassio, G.; Prangé, T.; David, H. N.; Santos, J. S. O.; Gabison, L.; Delcroix, N.; Abraini, J. H.; Colloc'h, N. Pressure-response Analysis of Anesthetic Gases Xenon and Nitrous Oxide on Urate Oxidase: A Crystallographic Study. *FASEB J.* **2011**, *25*, 2266–2275. https://doi.org/10.1096/fj.11-183046.

(25) Roose, B. W.; Zemerov, S. D.; Dmochowski, I. J. Xenon-Protein Interactions: Characterization by X-Ray Crystallography and Hyper-CEST NMR. *Methods Enzymol.* **2018**, *602*, 249–272. https://doi.org/10.1016/bs.mie.2018.02.005.

(26) Sauguet, L.; Fourati, Z.; Prangé, T.; Delarue, M.; Colloc'h, N. Structural Basis for Xenon Inhibition in a Cationic Pentameric Ligand-Gated Ion Channel. *PLoS One* **2016**, *11*, e0149795. https://doi.org/10.1371/journal.pone.0149795.

(27) Colloc'h, N.; Carpentier, P.; Montemiglio, L. C.; Vallone, B.; Prangé, T. Mapping Hydrophobic Tunnels and Cavities in Neuroglobin with Noble Gas under Pressure. *Biophys. J.* **2017**, *113*, 2199–2206. https://doi.org/10.1016/j.bpj.2017.10.014.

(28) Colloch, N.; Marassio, G.; Prangé, T. Protein-Noble Gas Interactions Investigated by Crystallography on Three Enzymes - Implication on Anesthesia and Neuroprotection Mechanisms. In *Current Trends in X-Ray Crystallography*; InTech, 2011. https://doi.org/10.5772/27966.

(29) Winkler, D. A.; Katz, I.; Farjot, G.; Warden, A. C.; Thornton, A. W. Decoding the Rich Biological Properties of Noble Gases: How Well Can We Predict Noble Gas Binding to Diverse Proteins? *ChemMedChem* **2018**, *13*, 1931–1938. https://doi.org/10.1002/cmdc.201800434.

(30) Winkler, D. A.; Warden, A. C.; Prangé, T.; Colloc'h, N.; Thornton, A. W.; Ramirez-Gil, J.-F.; Farjot, G.; Katz, I. Massive in Silico Study of Noble Gas Binding to the Structural Proteome. *J. Chem. Inf. Model.* **2019**, *59*, 4844–4854. https://doi.org/10.1021/acs.jcim.9b00640.

(31) Berman, H. M.; Westbrook, J.; Feng, Z.; Gilliland, G.; Bhat, T. N.; Weissig, H.; Shindyalov, I. N.; Bourne, P. E. The Protein Data Bank. *Nucleic Acids Res.* **2000**, *28*, 235–242. https://doi.org/10.1093/nar/28.1.235.

(32) George, D. G.; Barker, W. C.; Hunt, L. T. Mutation Data Matrix and Its Uses. *Methods Enzymol.* **1990**, *183*, 333–351. https://doi.org/10.1016/0076-6879(90)83022-2.

(33) Levitt, M. A Simplified Representation of Protein Conformations for Rapid Simulation of Protein Folding. *J. Mol. Biol.* **1976**, *104*, 59–107. https://doi.org/10.1016/0022-2836(76)90004-8.

(34) Quillin, M. L.; Breyer, W. A.; Griswold, I. J.; Matthews, B. W. Size versus Polarizability in Protein-Ligand Interactions: Binding of Noble Gases within Engineered Cavities in Phage T4 Lysozyme. *J. Mol. Biol.* **2000**, *302*, 955–977. https://doi.org/10.1006/jmbi.2000.4063.

(35) Abraini, J. H.; Marassio, G.; David, H. N.; Vallone, B.; Prangé, T.; Colloc'h, N. Crystallographic Studies with Xenon and Nitrous Oxide Provide Evidence for Protein-Dependent Processes in the Mechanisms of General Anesthesia. *Anesthesiology* **2014**, *121*, 1018–1027. https://doi.org/10.1097/ALN.0000000000000435.

(36) Krimmer, S. G.; Cramer, J.; Schiebel, J.; Heine, A.; Klebe, G. How Nothing Boosts Affinity: Hydrophobic Ligand Binding to the Virtually Vacated S1′ Pocket of Thermolysin. *J. Am. Chem. Soc.* **2017**, *139*, 10419–10431. https://doi.org/10.1021/jacs.7b05028.

(37) Lafumat, B.; Mueller-Dieckmann, C.; Leonard, G.; Colloc'h, N.; Prangé, T.; Giraud, T.; Dobias, F.; Royant, A.; van der Linden, P.; Carpentier, P. Gas-Sensitive Biological Crystals Processed in Pressurized Oxygen and Krypton Atmospheres: Deciphering Gas Channels in Proteins Using a Novel `soak-and-Freeze' Methodology. *J. Appl. Crystallogr.* **2016**, *49*, 1478–1487. https://doi.org/10.1107/S1600576716010992.

(38) Moschetti, T.; Mueller, U.; Schulze, J.; Brunori, M.; Vallone, B. The Structure of Neuroglobin at High Xe and Kr Pressure Reveals Partial Conservation of Globin Internal Cavities. *Biophys. J.* **2009**, *97*, 1700–1708. https://doi.org/10.1016/j.bpj.2009.05.059.

(39) Ardiccioni, C.; Arcovito, A.; Della Longa, S.; van der Linden, P.; Bourgeois, D.; Weik, M.; Montemiglio, L. C.; Savino, C.; Avella, G.; Exertier, C.; Carpentier, P.; Prangé, T.; Brunori, M.; Colloc'h, N.; Vallone, B. Ligand Pathways in Neuroglobin Revealed by Low-Temperature Photodissociation and Docking Experiments. *IUCrJ* **2019**, *6*, 832–842. https://doi.org/10.1107/S2052252519008157.

(40) Harris, K.; Armstrong, S. P.; Campos-Pires, R.; Kiru, L.; Franks, N. P.; Dickinson, R. Neuroprotection against Traumatic Brain Injury by Xenon, but Not Argon, Is Mediated by Inhibition at the *N* -Methyl- D -Aspartate Receptor Glycine Site. *Anesthesiology* **2013**, *119*, 1137–1148. https://doi.org/10.1097/ALN.0b013e3182a2a265.

(41) Tapper, D.; Arensman, R.; Johnson, C.; Folkman, J. The Effect of Helium-Oxygen Mixtures on Body Temperature. *J. Pediatr. Surg.* **1974**, *9*, 597–603. https://doi.org/10.1016/0022-3468(74)90094-3.

(42) David, H. N.; Haelewyn, B.; Chazalviel, L.; Lecocq, M.; Degoulet, M.; Risso, J.-J.; Abraini, J. H. Post-Ischemic Helium Provides Neuroprotection in Rats Subjected to Middle Cerebral Artery Occlusion-Induced Ischemia by Producing Hypothermia. *J. Cereb. Blood Flow Metab.* **2009**, *29*, 1159–1165. https://doi.org/10.1038/jcbfm.2009.40.

(43) Sano, Y.; Marty, B.; Burnard, P. Noble Gases in the Atmosphere. In *The Noble Gases as Geochemical Tracers*; Advances in Isotope Geochemistry; Springer: Berlin, Heidelberg, 2013; pp 17–31. https://doi.org/10.1007/978-3-642-28836-4_2.

(44) Elber, R.; Karplus, M. Multiple Conformational States of Proteins: A Molecular Dynamics Analysis of Myoglobin. *Science* **1987**, *235*, 318–321. https://doi.org/10.1126/science.3798113.

(45) Tilton, R. F.; Singh, U. C.; Weiner, S. J.; Connolly, M. L.; Kuntz, I. D.; Kollman, P. A.; Max, N.; Case, D. A. Computational Studies of the Interaction of Myoglobin and Xenon. *J. Mol. Biol.* **1986**, *192*, 443–456. https://doi.org/10.1016/0022-2836(86)90374-8.

(46) Hermans, J.; Shankar, S. The Free Energy of Xenon Binding to Myoglobin from Molecular Dynamics Simulation. *Isr. J. Chem.* **1986**, *27*, 225–227. https://doi.org/10.1002/ijch.198600032.

(47) Mann, G.; Hermans, J. Modeling Protein-Small Molecule Interactions: Structure and Thermodynamics of Noble Gases Binding in a Cavity in Mutant Phage T4 Lysozyme L99A11. *J. Mol. Biol.* **2000**, *302*, 979–989. https://doi.org/10.1006/jmbi.2000.4064.

(48) Liu, L. T.; Xu, Y.; Tang, P. Mechanistic Insights into Xenon Inhibition of NMDA Receptors from MD Simulations. *J. Phys. Chem. B* **2010**, *114*, 9010–9016. https://doi.org/10.1021/jp101687j.

Table of contents graphic